Lab on a Chip

Dynamic Article Links ►

Cite this: DOI: 10.1039/c2lc00000x

www.rsc.org/loc

PAPER

Microfluidic platform for culture and live cell imaging of cellular microarrays

Alexander Johnson,*[a] John Byce,*[a] Sarah Reichert,*[a] Anthony Sprangers,*[a] John Puccinelli,[a] and Randolph Ashton[a]

Received 9th May 2012
DOI: 10.1039/c2lc000000x

Dopamine (DA) is a neurotransmitter that controls motor movement. Patients who suffer from Parkinson's disease (PD) have deficiencies in their neurons that synthesize and release DA. Current therapies for PD lessen symptoms by supplementing the lost dopamine; this improves patient quality of life but does not treat the underlying disease mechanisms. Neural stem cells (NSCs) have the potential to regenerate lost neurons and restore healthy dopamine levels in PD patients due to their ability to differentiate into all types of neurons. Differentiation of NSCs *in vivo* is primarily regulated through the localization and concentration of soluble molecules in the cellular microenvironment; microfluidic devices can be used to replicate this process in an *in vitro* setting. Here, we adapted and fabricated a microfluidic device, originally devised by Jeon *et al*., that utilizes seven Christmas tree structures to generate an array of discrete concentrations of soluble molecules. By integrating this system to flow concentrations over a cellular microarray, the effects of various factors on NSC differentiation can be tested in a high-throughput and temporally dynamic manner. This will enable efficient identification of mechanisms related to the differentiation of dopaminergic neurons, and ultimately produce a homogenous population of neurons for regenerative medicine therapies.

Introduction

The limited amount of cell proliferation in the mature nervous system is devastating for patients with neurodegenerative diseases resulting from the loss of neuron structure and function.[1] This is especially true with Parkinson's disease (PD), which is caused by the loss of dopaminergic neurons in the midbrain.[2] Patients with PD experience tremors, compromised coordination, and other diminished motor functions that decrease their quality of life.[2] The National Institute of Health estimates that approximately 500,000 Americans currently suffer from PD, with another 50,000 new incidences occurring annually.[3] Presently, there is no cure for PD; current therapies treat the symptoms without correcting the underlying neuron loss.[1] Fortunately, recent research suggests a regenerative therapy approach may be appropriate, as neural stem cells (NSCs) have been shown to differentiate into all the neuron types present in the nervous system.[1] One of the factors that determines NSC fate *in vivo* is the exposure to concentration gradients of soluble factors, such as fibroblast growth factor (FGF), sonic hedgehog (Shh), Wnt, and bone morphogenic proteins (BMPs).[4] Based on the position of a cell within the gradient, gene expression, and subsequently cell fate, can be tightly controlled.[4] Although this approach is promising, many of the factors that induce specific NSC lineage differentiation need to be identified and examined before this becomes a viable treatment option.

Using standard cell culture techniques to test for optimal soluble factor concentrations would be extremely expensive and time consuming. A more high-throughput method for accomplishing this involves the implementation of microfluidics. Previous studies have demonstrated that various microfluidic devices can generate accurate, reproducible concentration gradients of soluble molecules.[5-11] Microfluidics have the additional benefit of being able to be integrated with clonal microarrays, which consist of hundreds to thousands of separate cell colonies seeded onto a patterned surface.[12] Microarrays allow for the high-throughput, simultaneous analysis of many conditions when incorporated into a gradient-generating microfluidic device. Following testing, individual cell colonies can be recovered, expanded with standard cell culture techniques, and examined using biological assays to analyze cell fates.[12]

Manipulating flow rates of fluids in microfluidic devices can alter the flow regimes. The dominant flow regime depends on the value of the dimensionless Peclet (Pe) number, which determines the balance between convection and diffusion.[13] If Pe >> 1, convective flow dominates and any soluble factors released by cells within the microfluidic device are swept away by the convective fluid flow, minimizing paracrine and autocrine signaling. However, if Pe < 1, diffusion dominates convection and paracrine and autocrine signaling can occur.[13] Therefore, the ability to include autocrine and paracrine signaling in microfluidic devices is easily tailored based on the input velocity and corresponding Peclet number.

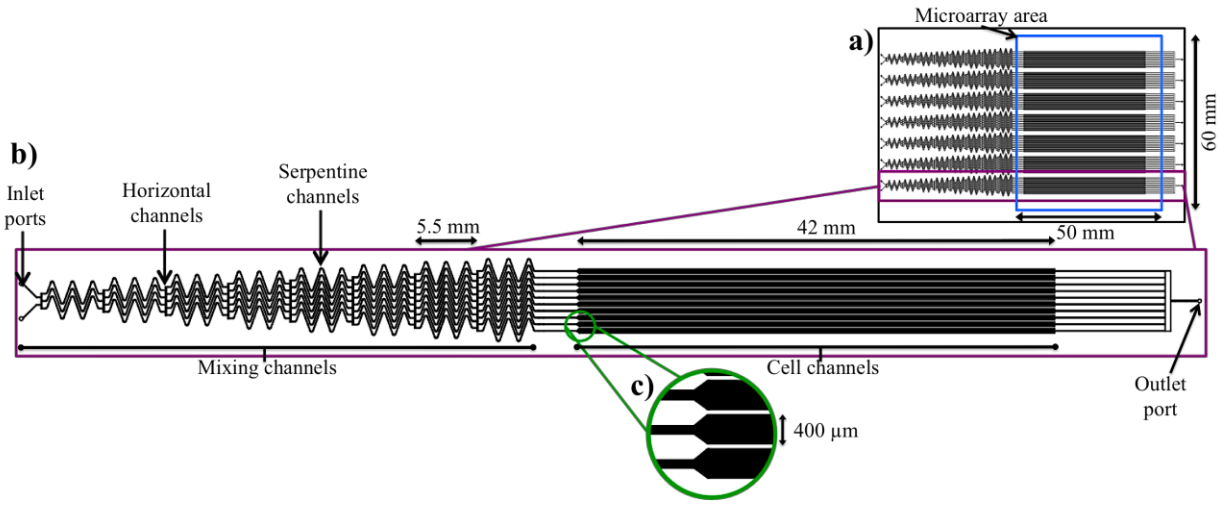

Figure 1: a) Complete concentration array generation system showing the location of where the glass coverslip with the cellular microarray will be placed. **b)** Magnification of one Christmas tree structure indicating the important features of the design. **c)** Further magnification of where the mixing channels convert to the singular concentration channels that will flow fluids over the cellular microarray.

Another important dimensionless variable to consider when manipulating flow regimes is the Peclet-number-to-Damkohler-number ratio. The Damkohler (Da) number determines the balance between diffusion and ligand reaction with the cell receptor. Consequently, the Pe/Da ratio determines the balance between convection and ligand reaction with the receptor.[13] Convection dominates ligand-receptor reaction when Pe/Da >> 1, which supports minimizing autocrine and paracrine signaling. If Pe/Da ~ 1, then ligand-receptor reaction will occur before convective flow removes ligands from the cell surface.[13]

Following the Christmas tree design first established by Jeon *et al*.[11] to create a concentration array generator, we fabricated a platform that integrates this microfluidic device with a cellular microarray for examining NSC responses to soluble factors. This system allows for high-throughput analysis with reduced costs and reagent quantities, efficient manipulation of fluids, and beneficial fluid characteristics, such as laminar flow. With this platform, we hope to be able to determine the specific soluble factor concentrations necessary to elicit NSC differentiation down specific neuronal lineages. This knowledge can then be applied to direct controlled differentiation of NSCs for use in regenerative therapies.

Materials and methods

Microfluidic device description

Our microfluidic device contains seven Christmas tree concentration array generators, as shown in Figure 1. A negative-replica silicon master was fabricated with 200-µm high SU-8 100 features (MicroChem, Newton, MA) following the manufacture's protocol.[14] The polydimethyl siloxane (PDMS) mold for the experimental device was made using soft lithography techniques.[14] Briefly, 184 Silicone Elastomer base and curing agent (Dow Corning, Midland, MI) were mixed at a 10:1 base-to-curing-agent ratio to generate the mold solution. This solution was poured on top of the negative silicon master and placed in a vacuum chamber, where a vacuum was pulled for approximately 30 minutes. Next, the PDMS was cured at 100 °C for 1 hour. Plasma oxidization was used to bind the PDMS to a 1.0-mm thick glass piece for experimentation.

Computational analysis and statistics

A theoretical simulation of the concentration array generation was conducted using COMSOL Multiphysics 4.2 (Comsol Inc., Los Angeles, CA) software. This analysis was performed using the microfluidics module with creeping flow and transport of diluted species modeling. Creeping flow was velocity-driven using a variable input flow rate of incompressible fluid.

For the fluorescence comparison and convection flow analysis, an input velocity of 1.67 mm/s, which corresponds to a volumetric flow rate of approximately 1 µL/min, was used. For flow allowing reaction and diffusion, modeling was done with an input flow rate of 7.85×10^{-4} mm/s. The transport of diluted species analysis was coupled to the velocity inflow from the creeping flow model. A linear solver was used to calculate the theoretical concentration gradient using an "extremely fine" general physics, tetrahedral mesh. Graphing and statistical analyses were conducted using Sigma Plot (Systat Software Inc., San Jose, CA).

Fluorescence imaging

The microfluidic device was utilized to generate concentration arrays that were examined with a fluorescence microscope. Solutions of 0 µM and 25 µM fluorescein isothiocyanate (FITC)-labeled dextran (40 kDa, Sigma Aldrich, St. Louis, MO) were injected into the two inlets of one Christmas tree structure at flow rates of 1.0 µL/min. A concentration array was generated and allowed to equilibrate for over 10 minutes. The device was imaged with an Olympus 1X81 Environmental Microscope (Olympus Valley Inc., Center Valley, PA) using cellSens Dimension software (Olympus Valley Inc., Center Valley, PA). FITC intensity analysis was conducted using ImageJ (free source)

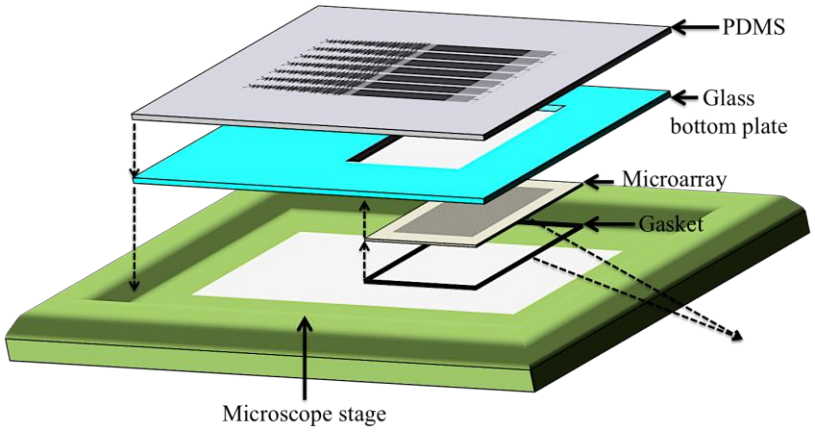

Figure 2: The PDMS mold containing the concentration array generator was plasma oxidized to the glass bottom plate. This glass piece had a cutout section to allow for the integration of the gold-coated glass piece with the cellular microarray. The microarray was aligned with an electronic aligner and inserted from underneath, followed by a gasket and sealant to secure it in place during imaging and experimentation. After experiments were complete, the gasket and sealant were taken out to remove the microarray.

software. Three regions of interest were chosen in each cell channel and an average intensity was determined from them. A standard curve was developed to relate intensity to concentration of FITC-dextran. Six samples (0 μM, 5 μM, 10 μM, 15 μM, 20 μM, and 25 μM) were created through serial dilutions and a single standard concentration was pushed through the microfluidic device for imaging and analysis to determine the corresponding intensity. The same exposure rate was used for standards and experimental samples. Ethanol was washed through the device between samples.

Integration

As shown in Figure 2, the surfaces of the PDMS and glass bottom plate were plasma oxidized and aligned so that the cell channels of the concentration array generator were arranged above the opening for the clonal microarray. The microarray was then aligned from underneath and inserted along with a gasket and temporary sealant to secure it in place and prevent the device from leaking at the glass interfaces. After experimentation, the sealant was peeled away and the gasket was removed in order to take out the microarray and enable the colonies to be expanded and analyzed for induced cell fates.

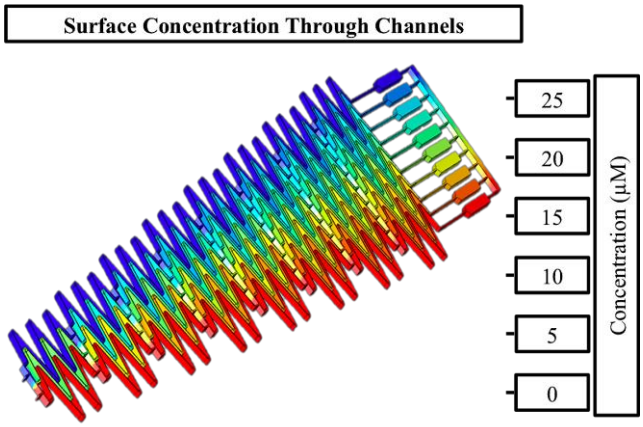

Figure 3: COMSOL three-dimensional computational model showing diffusive mixing in the serpentine channels.

Results and discussion

Computational analysis and statistics

The concentration gradient computed by the COMSOL analysis was consistent with what was expected based on previous descriptions in literature.[11] As depicted in Figure 3, the model demonstrated diffusive mixing in the serpentine channels of the microfluidic device. The final concentrations generated are shown in Figure 4, normalized to the maximum concentration for ease of comparison with experimental results. The concentration gradient generated by the COMSOL simulation adhered to an expected binomial trend with an R^2 value of 0.996 and accurately predicts the concentrations of the constructed Christmas tree gradient for flow rates up to 1.67 mm/s (1 μL/min). This flow rate was verified for adequate diffusion of bovine serum albumin in the serpentine channels using transport equations (see supplementary information, *Diffusion within Serpentine Channels*).

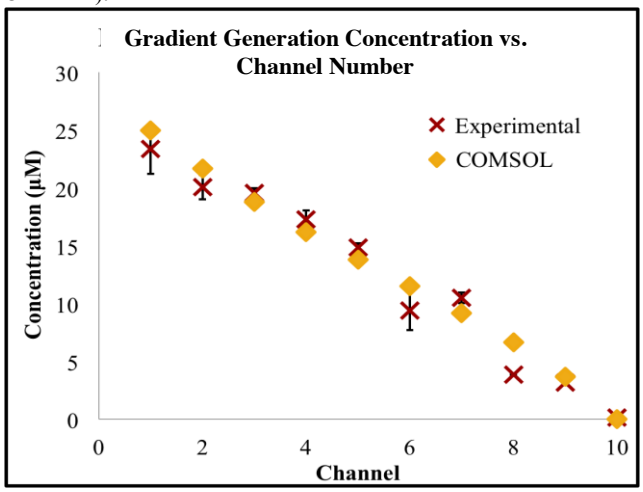

Figure 4: Normalized concentrations from computational analysis and experimental testing. The computational analysis follows a binomial trend, and the experimental testing adheres closely to this except for channels six and eight. These discrepancies may have resulted from increased resistances in the upstream channels, which altered fluid flow through the system.

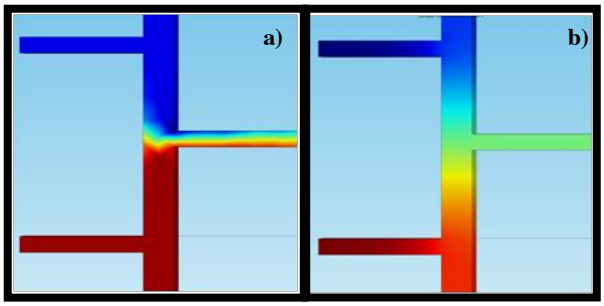

Figure 5: a) Convective-dominated flow regime (Pe=74, Pe/Da=1254). Distinct concentration streams are maintained for a significant distance into the next serpentine channel. **b)** Diffusion/reaction dominated flow regime (Pe=0.05, Pe/Da=1). Diffusive mixing occurs in the horizontal channel. Depending on the input flow, a prediction can be made as to whether the flow will be convective or diffusion/reaction-dominated. This determines whether or not autocrine and paracrine signalling can occur between the cells in the cell channels. These flow regimes can be modelled using the COMSOL software, allowing for the determination of soluble factor concentrations exposed to cells.

Using COMSOL, flow in both the convection-dominant and diffusion-reaction regime can be accurately modeled. Figure 5a is a depiction of channel mixing in a convection-dominant regime (Pe=74, Pe/Da =1254). Distinct concentration streams retain their integrity for a significant distance down mixing channels. Flow in a diffusion and reaction regime (Pe=0.05, Pe/Da=1), as seen in Figure 5b, is characterized by diffusive mixing prior to the mixing channel itself. As a result, the overall gradient generated depends on the input flow parameters. The COMSOL simulation enables theoretical predictions of the gradient generated in all flow regimes, allowing for characterization of experimental results.

Fluid shear stress on cells

Through COMSOL analysis and manual calculations (see supplementary information, *Diffusion within Serpentine Channels*), the maximum fluid shear stress on each individual cell in the cell channels was determined to be 0.021 dynes/cm^2. This is an order of magnitude lower than what is considered to be low cell shear stress, meaning no adverse effects will be imposed on the cells by shear stress while fluids are flowing through the device.[13]

Fluorescence imaging

The concentration gradient generated in the experimental device is shown in Figure 4. The concentration in each channel was calculated based on the standard curve relating fluorescence intensity and concentration (data not shown). These values were normalized to the maximum concentration for ease of comparison with computational results. The developed concentration array was consistent with the COMSOL analysis, suggesting the device functioned in accordance with the predictions made in the simulation. However, channels six and eight were slightly lower than predicted. This may have been due to an obstruction in the channels upstream of where the measurements were taken, which would have altered the channel resistances and subsequently fluid flow.

Conclusions

Here, a microfluidic concentration array generator was designed and fabricated. Computational and experimental arrays were developed and found to yield consistent results. Now that functionality has been confirmed, the experimental device can be integrated with a cellular microarray for the high-throughput analysis of soluble factor concentrations on inducing NSCs to differentiate into dopaminergic neurons. Hopefully this will help elucidate optimum factor concentrations and combinations for specific and efficient homogeneous differentiation of NSCs. This device has the potential to be expanded to applications for studying other stem cells fates as well as drug screening to determine optimal dose concentrations.

Notes and references

[*] *These authors contributed equally to this work*
[a] *Department of Biomedical Engineering, University of Wisconsin-Madison, Madison, WI 53706, USA. E-mail: adjohnson5@wisc.edu; byce@wisc.edu; sreichert@wisc.edu; ajsprangers@wisc.edu*

1 NIH. (2005, *The Life and Death of a Neuron*. Available: http://www.ninds.nih.gov/disorders/brain_basics/ninds_neuron.htm
2 NINDS. (2004, *Parkinson's Disease Backgrounder*. Available: http://www.ninds.nih.gov/disorders/parkinsons_disease/parkinsons_disease_backgrounder.htm
3 NIH. (2006, *Parkinson's Disease: Hope Through Research*. Available: http://www.ninds.nih.gov/disorders/parkinsons_disease/detail_parkinsons_disease.htm
4 J. L. S. Tomas Vacik, Greg Lemke. (2011, *The Battle of the Morphogens: How to Get Ahead in the Nervous System*. Available: http://neurosciencenews.com/morphogens-brain-development-wnt-vax-tcf712/
5 N. L. Jeon, *et al*., "Generation of solution and surface gradients using microfluidic systems," *Langmuir*, vol. 16, pp. 8311-8316, 2000.
6 N. L. Jeon, *et al*., "Microfluidic gradient devices," ed: Google Patents, 2011.
7 S. K. W. Dertinger, *et al*., "Generation of gradients having complex shapes using microfluidic networks," *Analytical Chemistry*, vol. 73, pp. 1240-1246, 2001.
8 D. J. Beebe and V. V. Abhyankar, "Microfluidic platform and method of generating a gradient therein," ed: Google Patents, 2008.
9 T. M. Keenan, *et al*., "Microfluidic "jets" for generating steady-state gradients of soluble molecules on open surfaces," *Applied physics letters*, vol. 89, p. 114103, 2006.
10 S. K. Sia and G. M. Whitesides, "Microfluidic devices fabricated in poly (dimethylsiloxane) for biological studies," *Electrophoresis*, vol. 24, pp. 3563-3576, 2003.
11 S. Kim, *et al*., "Biological applications of microfluidic gradient devices," *Integr. Biol*., 2010.
12 R. S. Ashton, *et al*., "High Throughput Screening of Gene Function in Stem Cells Using Clonal Microarrays," *Stem Cells*, vol. 25, pp. 2928-2935, 2007.
13 L. M. Przybyla and J. Voldman, "Attenuation of extrinsic signaling reveals the importance of matrix remodeling on maintenance of embryonic stem cell self-renewal," *Proceedings of the National Academy of Sciences*, vol. 109, pp. 835-840, 2012.

14 Microchem, "Negative Tone Photoresist Formulations 50-100," ed, 2002.

5

Supplementary Information: Transport equations for adequate diffusion and fluid shear stress

Diffusion within serpentine channels

Diffusion through the serpentine channels was modeled using COMSOL which was then verified using transport phenomena equations. We chose to use bovine serum albumin (BSA) as a model protein due to its large size (66.4 kDa).[1] We will be using proteins that are smaller than BSA, so BSA is modeling a very maximal situation. The diffusion coefficient of BSA is reported to be D = 6.81 x 10^{-11} m^2/s.[2] Diffusion follows Fick's law, relating the velocity vector of the fluid to the diffusion coefficient and concentration gradient, which can be seen as equation 1.[3]

Equation 1- $$\frac{\partial C_A}{\partial t} + (v \cdot \nabla C_A) = D * \nabla^2 C_A$$

This is greatly simplified if diffusion is present in only one direction. Luckily, in our case diffusion is only important in the direction perpendicular, but in the same plane as the flow. Using this simplification, it is easy to solve for the time it takes particles to diffuse from the boundary layer of two neighboring streams, to the opposite channel wall. This equation can be seen as equation 2.[2,4]

Equation 2- $$t = \frac{d^2}{D}$$

Here, d is the distance to diffuse and D is the diffusion coefficient. Applying this to our microfluidic device where d = 50 microns (50 microns divided by two is 25 microns, which is technically the distance a molecule needs to travel since there are two neighboring streams in one channel; however, modeling the diffusive distance as 50 microns gives us a safety factor of two built in) and D = 6.81 x 10^{-11} m^2/s (BSA diffusivity) yields a time of 9.18 seconds for the establishment of diffusion equilibrium. Since we know the flow rate of our fluid, we can determine how far this mixing stream will travel down the serpentine channel using the diffusion time reported above. We can then compare this distance to the known distance of a single serpentine channel, which is 10.55mm. If the distance traveled by the mixing fluid is less than the distance of a serpentine channel, then we know the flow rate will allow for adequate diffusion of molecules in the serpentine channel before the next branching point. However, if the distance traveled by the mixing fluid is greater than the length of a serpentine channel, then we need to lower the flow rate to allow for more time in the serpentine channel for adequate diffusion.

Since our device utilizes two inputs at an equal flow rate, the greatest flow rate will be in the first branch of serpentine channels (since the two input flow rates divide into three serpentine channels, each serpentine channel will have a flow rate equal to 2/3 the input flow rate). Further branching within the Christmas tree gradient generator will result in a decreased flow rate for each successive branching level, which will allow for more time for diffusion. Thus, it is appropriate to model the diffusion solely within the first three serpentine channels since these will experience the least time to achieve diffusion equilibrium as they experience the greatest flow rate.

A flow rate of 0.685 $\boldsymbol{\mu}$L/minute resulted in a distance traveled of 10.48 mm by the mixing fluid. This is the maximum flow rate which still allows for proper diffusion within the length of a single serpentine channel (since 10.48 mm is less than 10.55 mm). This translates to an inlet flow rate of 1.0275 $\boldsymbol{\mu}$L/minute.

Fluid shear stress on cells

In pressure-driven flow systems, such as our microfluidic device, the pressure drop, ΔP, is related to the volumetric flow rate, Q, and fluid resistance, R, via equation 3.[3,5]

Equation 3- $$\Delta P = Q * R$$

In our specific system the cell culture channels have a rectangular cross-section. Fluid resistance for this type of cross-section is described by equation 4.[4-5]

Equation 4- $$R = \frac{12*\mu*L}{h^2*w\left(1-\frac{192}{\pi^5*w}*\sum_{n=0}^{\infty}\frac{\tanh\left((2*n+1)\frac{\pi*w}{2*h}\right)}{(2n+1)^5}\right)}$$

Here, h = channel height, w = channel width, L = channel length and $\boldsymbol{\mu}$ = fluid viscosity. For simplicity, this can be modeled using equation 5.

Equation 5- $$R = \frac{12*\mu*L}{w*h^3}$$

We assumed our flow profile through the cell culture channels would be well-approximated by laminar flow through a narrow slit. The velocity profile through this type of slit is described by equation 6.[3]

Equation 6- $$V_y(x) = \frac{\Delta P*w^2}{2*\mu*L}\left[1-\left(\frac{x}{w}^2\right)\right]$$

Using Newton's law of viscosity[3] (equation 7) we can solve for the momentum flux, $\boldsymbol{\tau}$.

Equation 7- $$\tau = -\mu * \frac{dV_y}{dx}$$

Substituting equation 6 into equation 7 and taking the derivative of the velocity profile allows us to solve for the max shear stress which occurs at the channel wall, i.e. when x = w (can assume this because we are assuming a "no-slip" condition at the wall, meaning the fluid at the wall is not moving). This results in equation 8.

Equation 8- $$\tau_{max} = \frac{12*\mu*Q}{h^3}$$

Using this final equation, the viscosity of water, h = 130 microns (the cell channel is 200 microns tall but we are assuming there is a cellular colony seven cells high on a pixel, each cell being 10 microns high), and the flow rate discussed in the above diffusion section, cells in this type of system would experience a maximal shear stress of 0.021 dynes/cm^2. This is an order of magnitude lower than what is considered low cell shear stress[6] and is two orders of magnitude below typical physiological shear stresses experience by endothelial cells during normal blood flow which is approximately 2 dynes/cm^2.[7] Thus, adverse affects due to shear stress should not be a problem in this design.

Notes and references

1 Sigma-Aldrich. (1997, *Albumin, Bovine*. Available: http://www.sigmaaldrich.com/etc/medialib/docs/Sigma/Product_Information_Sheet/a4919pis.Par.0001.File.tmp/a4919pis.pdf

2 C. Geankoplis, *Transport Processes and Unit Operations*, Third ed., 1993.
3 S. Bird, *Transport Phenomena Revised Second Edition*: John Wiley & Sons, 2007.
4 D. J. Beebe, *et al*., "Physics and applications of microfluidics in biology," *Annual review of biomedical engineering*, vol. 4, pp. 261-286, 2002.
5 L. Kim, *et al*., "Microfluidic arrays for logarithmically perfused embryonic stem cell culture," *Lab Chip*, vol. 6, pp. 394-406, 2006.
6 L. M. Przybyla and J. Voldman, "Attenuation of extrinsic signaling reveals the importance of matrix remodeling on maintenance of embryonic stem cell self-renewal," *Proceedings of the National Academy of Sciences*, vol. 109, pp. 835-840, 2012.
7 B. G. Chung and J. Choo, "Microfluidic gradient platforms for controlling cellular behavior," *Electrophoresis*, 2010.